

# Powder Diffraction (BL02B2)

## 1. Introduction

A BL02B2 beamline was designed and constructed for research on accurate crystal structure analysis using powder diffraction data in fiscal year 1998. The idea for experiments at the beamline was basically proposed by Professor Makoto Sakata of Nagoya University and his Accurate Structure for Material Science Group. The purpose and details of the experiments are described elsewhere [1,2]. Since the user group requested a high-parallel and high-energy resolution beam to obtain high-resolution powder diffraction data, the beamline optics starts with a parabola-shape mirror followed by a double-crystal monochromator (Fig. 1). The first beam time between June and December 1999 was mainly dedicated to tuning up the beamline and trial experiments. The characteristic performance of the beamline has been cleared by the adjustment of beamline components and optical elements. This paper presents the current status of the optical station in the BL02B2 beamline.

## 2. Optics and Performance

### 2.1 Light source

The light source of the beamline is a B2-type bending magnet that has its magnetic field at 0.679T and critical energy at 28.9keV. The white X-ray generated by the bending magnet is introduced into a quadrant slit in an optical hutch and is orthopediated into a typical dimension of 1.8mm(V) $\times$ 1.0mm(H) to remove excess X-ray beams which increase the heat load on the next optical element.

### 2.2 Energy Resolution

A high-parallel and high-energy resolution X-ray beam is required for the powder diffraction experiments at the beamline. We placed a parabola-shape mirror upstream of a monochromator to make a parallel beam incident on the crystal in the monochromator. The function of the mirror is not only the collimation of the X-ray beam but also 1. rejection of high-energy harmonics, 2. reduction of the heat load on the first crystal in the monochromator, and 3.

the focusing of the X-ray beam. The parabola-shape is configured by bending a 1m flat mirror using a stepping-motor actuator [3]. The figure of the mirror surface is a good approximation of the ideal parabola-shape in the case of a very small curvature. The most appropriate bending condition is investigated by measuring crystal rocking curves in dispersive geometry. The minimum width of the rocking curve corresponds to the highest energy resolution, thus giving the most appropriate bending condition (Fig. 2). By using the collimating mirror, the energy resolution improved several times. Especially in case of Si 311 crystal, ca.  $3 \times 10^{-5}$  of high-energy resolution ( $\Delta E/E$ ) close to a theoretical limit is available in the experimental hutch, although the photon flux drastically decreases.

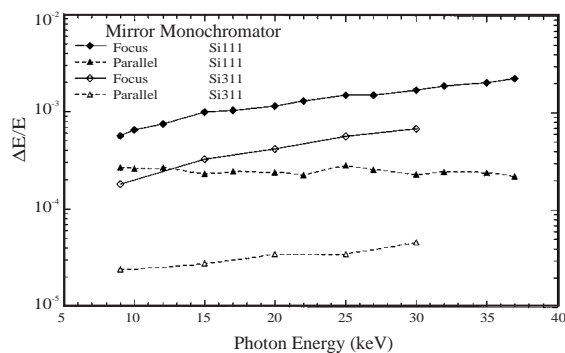


Fig. 2. Energy resolution.

### 2.3 Focus

The bending of the mirror also makes available X-ray beams focused in a vertical direction, if the user requires a high photon flux instead of high-energy resolution. The bending condition is adjusted by observations of the focus image at the experimental hutch. The FWHM of the X-ray beam along the vertical direction becomes smaller than 0.2mm at the sample position, though it requires a very tight controlled to obtain fine focusing (Fig. 3). It was also observed that changing the radius of curvature using the bending mechanism dose not cause any significant change in the beam position. The flux density at the fine focus increased by 8 times larger compared to when the mirror was flattened.

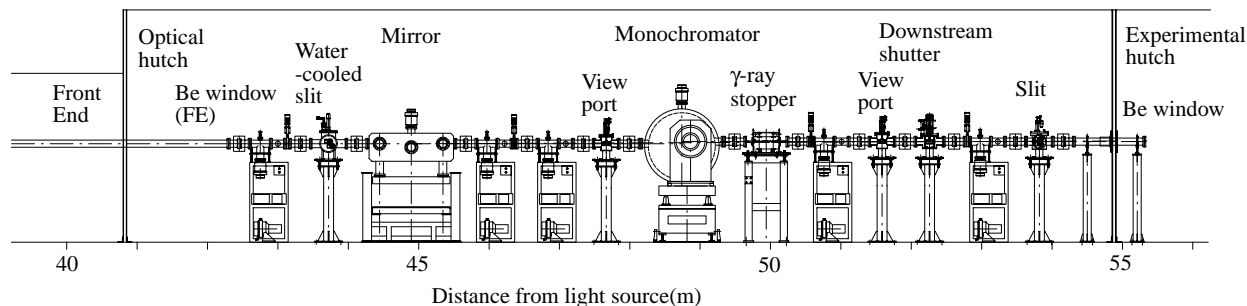


Fig. 1. Schematic view in the optical hutch of the BL02B2 beamline.

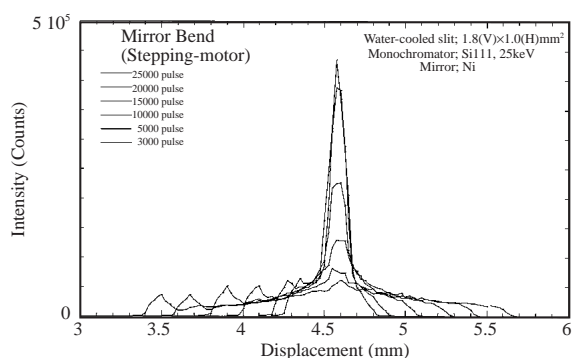


Fig. 3. Distribution of the incident X-rays focused by mirror, obtained by a vertical scan of a  $0.1 \times 0.1 \text{ mm}^2$  slit at the experimental hutch.

#### 2.4 Rejection of Higher Harmonics

In the BL02B2 beamline, the glancing angle cannot be changed because of the arrangement of the components, such as the mirror and the monochromator. In addition, a small glancing angle of 2.0 mrad was adopted, since a user group requested high photon energy to decrease the correction of X-ray absorption at the sample. Cut-off energy, in which a reflectivity of the total reflection mirror drastically varies as a function of photon energy, is approximately a function of the glancing angle and the density of the mirror surface in the case of hard X-rays. In order to select cut-off energy, two elements of Pt and Ni are coated on a Si substrate (Fig. 4). A user can easily choose the cut-off energy among those of Pt, Ni, and Si (substrate) by horizontal translation of the mirror perpendicular to the beam axis. Cut-off energy is observed at 37keV, 28keV, and 16keV at Pt, Ni, and Si, respectively. Thus small harmonics contaminant less than  $10^{-2}$  is available. It was observed that the incident X-rays introduced into the experimental hutch has a sufficient width of about 7mm.

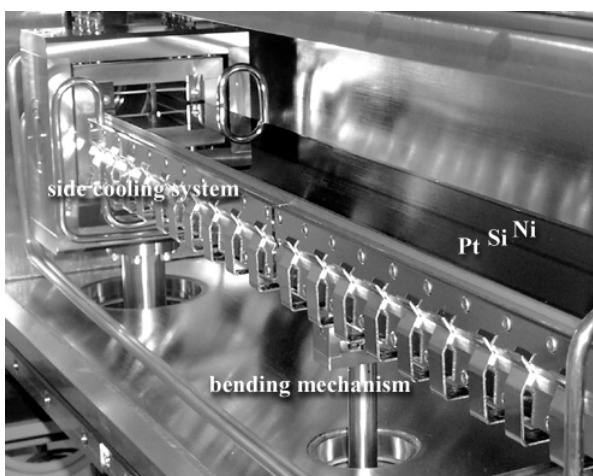


Fig. 4. Photograph of mirror.

#### 2.5 Photon Flux

A standard fixed-exit inclined double-crystal monochromator for a bending magnet beamline [4] has been adopted in the beamline. In the monochromator, a net plane of crystal can be switched among Si111, Si3111, and Si511 without breaking the vacuum chamber. An adequate net plane can be selected by estimating photon flux, energy resolution, and photon energy (see Table 1). It was thought that the heat load on the first crystal would be drastically reduced by the cut-off effect on a total reflection mirror. The heat load is not severe, thus allowing an indirect water-cooled method to be used for the first crystal. A flat Si crystal ( $90(\text{W}) \times 70(\text{D}) \times 10(\text{H}) \text{ mm}^3$ ) fabricated from an FZ Si ingot was adopted to avoid a photon flux reduction by strain and/or deformation caused by machining. The Si crystal is cooled through the copper holders by a so-called indirect cooling method (Fig. 5). The photon flux and flux density were measured using an ionization chamber at a Be window position and sample position in the experimental hutch, respectively (Fig. 6). The observed photon flux is almost consistent with the calculation made from an incident X-ray spectrum and the absorption of a graphite filter; Be window, air, and Kapton.

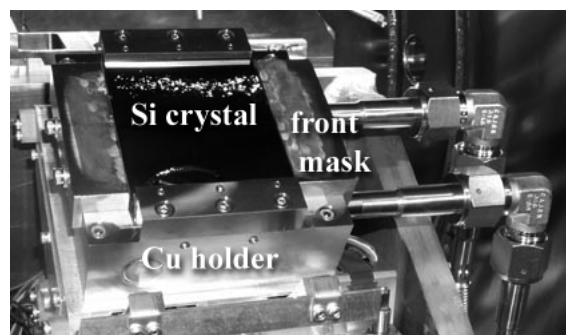


Fig. 5. Photograph of the first crystal in the monochromator.

A comparison between photon fluxes observed using two coatings of platinum is shown in Fig. 7. One is the first mirror coating before January 2000 and the other is the repaired one. The great difference between the cut-off energies was easily observed. It is thought that the low cut-off energy is caused by a low-density ratio against that of bulk platinum. In the previous mirror, a low-density ratio of about 40% is calculated using a graded index method of mirror reflectivity [5], in spite of 82% in the present mirror. Much effort, time, and money was spent in examination and to repair the previous coating. Details of the failure on the coating are now being researched by the supplier, CANON Inc.

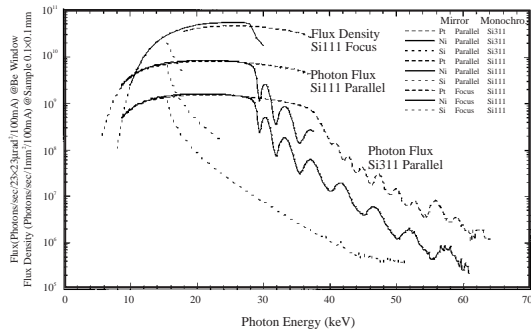


Fig. 6. Photon flux and flux density.

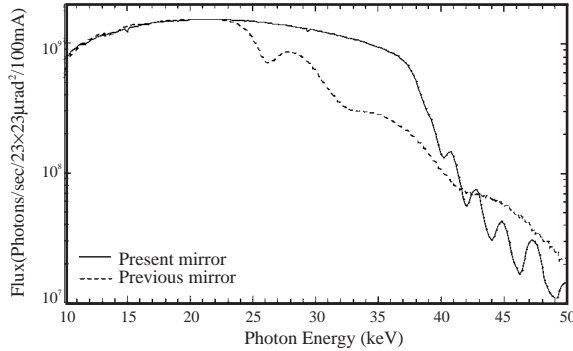


Fig. 7. Comparison between mirror coatings.

### 3. Summary

It becomes clear that a user can select an adequate net plane, a bending condition of the mirror, and the mirror surface by estimating the photon flux, energy resolution, and photon energy. It is clarified that the present status exceeds the design values of the performance specifications. No fluctuation in the intensity of the monochromatic beam was observed. The beamline facilities have been stably opened to users. The beamline can provide high quality synchrotron radiation for powder diffraction users.

### References

- [1] SPring-8 Annual Report 1998 (1998) 47.
- [2] E. Nishibori *et al.*, Proc. SRI2000 (2000).
- [3] T. Uruga *et al.*, Proc. SRI2000 (2000).
- [4] M. Yabashi *et al.*, Proc. SPIE **3773** (1999) 2.
- [5] S. Goto *et al.*, Rev. Sci. Instrum. **63** (1992) 1160.

Table 1. Summary of the BL02B2 beamline

Light Source	
Type	Bending magnet (B2-type)
Critical energy	28.9keV
Source size	$\sigma_x = 0.18$ mm $\sigma_y = 0.06$ mm $\sigma_y = 0.06$ mrad(@10keV)
Horizontal beam divergence	0.73mrad

### Facilities in Experimental Station

#### (i) Measurement

Debye-Sherron camera

Recording media; Imaging Plate

Radius of camera; 286.5mm

Offline IP reader

Gas-flow type ion chamber

#### (ii) Sample

Cryostat

Control range of temperature; 15~300K

High temperature gas flow system

Control range of temperature; 15~300K

### X-rays at Experimental Hutch

Energy (keV)	Flux (ph/s/100mA/0.1x0.1mm <sup>2</sup> )	Flux <sub>3rd</sub> /Flux <sub>1st</sub>	$\Delta E/E$	Mirror	Monochromator
10	5.7x10 <sup>6</sup>	1x10 <sup>-2</sup>	2.5x10 <sup>-5</sup>	Si, Parallel	Si311
15	1.1x10 <sup>7</sup>	3x10 <sup>-4</sup>	2.8x10 <sup>-5</sup>	Si, Parallel	Si311
20	1.2x10 <sup>7</sup>	2x10 <sup>-4</sup>	3.5x10 <sup>-5</sup>	Ni, Parallel	Si311
25	1.2x10 <sup>7</sup>	7x10 <sup>-5</sup>	3.5x10 <sup>-5</sup>	Ni, Parallel	Si311
30	9.7x10 <sup>6</sup>	4x10 <sup>-5</sup>	4.6x10 <sup>-5</sup>	Pt, Parallel	Si311
35	7.3x10 <sup>6</sup>	1x10 <sup>-5</sup>	5. x10 <sup>-5</sup>	Pt, Parallel	Si311
10	2.9x10 <sup>7</sup>	1x10 <sup>-2</sup>	2.6x10 <sup>-4</sup>	Si, Parallel	Si111
15	5.6x10 <sup>7</sup>	3x10 <sup>-4</sup>	2.3x10 <sup>-4</sup>	Si, Parallel	Si111
20	6.3x10 <sup>7</sup>	2x10 <sup>-4</sup>	2.4x10 <sup>-4</sup>	Ni, Parallel	Si111
25	6.3x10 <sup>7</sup>	7x10 <sup>-5</sup>	2.8x10 <sup>-4</sup>	Ni, Parallel	Si111
30	5.3x10 <sup>7</sup>	4x10 <sup>-5</sup>	2.3x10 <sup>-4</sup>	Pt, Parallel	Si111
35	4.2x10 <sup>7</sup>	1x10 <sup>-5</sup>	2.4x10 <sup>-4</sup>	Pt, Parallel	Si111
10	2.4x10 <sup>7</sup>	1x10 <sup>-2</sup>	6.5x10 <sup>-4</sup>	Si, Focus	Si111
15	2.6x10 <sup>8</sup>	3x10 <sup>-4</sup>	1.0x10 <sup>-3</sup>	Si, Focus	Si111
20	4.8x10 <sup>8</sup>	2x10 <sup>-4</sup>	1.2x10 <sup>-3</sup>	Ni, Focus	Si111
25	5.4x10 <sup>8</sup>	7x10 <sup>-5</sup>	1.5x10 <sup>-3</sup>	Ni, Focus	Si111
30	4.3x10 <sup>8</sup>	4x10 <sup>-5</sup>	1.7x10 <sup>-3</sup>	Pt, Focus	Si111
35	3.3x10 <sup>8</sup>	1x10 <sup>-5</sup>	2.0x10 <sup>-3</sup>	Pt, Focus	Si111